CRYSTALLIZATION AND MUTATIONAL STUDIES OF CARBON MONOXIDE DEHYDROGENASE FROM *Moorella thermoacetica*

A Thesis

by

EUN JIN KIM

Submitted to the Office of Graduate Studies of
Texas A&M University
in partial fulfillment of the requirements for the degree of

MASTER OF SCIENCE

May 2004

Major Subject: Chemistry

CRYSTALLIZATION AND MUTATIONAL STUDIES OF CARBON MONOXIDE DEHYDROGENASE FROM *Moorella thermoacetica*

A Thesis

by

EUN JIN KIM

Submitted to Texas A&M University
in partial fulfillment of the requirements
for the degree of

MASTER OF SCIENCE

Approved as to style and content by:

Paul A. Lindahl (Chair of Committee)	Frank M. Raushel (Member)
Marcetta Y. Darensbourg (Member)	James C. Sacchettini (Member)
Emile A. Schweikert (Head of Department)	

May 2004

Major Subject: Chemistry

ABSTRACT

Crystallization and Mutational Studies of Carbon Monoxide Dehydrogenase from *Moorella thermoacetica*. (May 2004)

Eun Jin Kim, B.S.; M. Ed., Korea National University of Education

Chair of Advisory Committee: Dr. Paul A. Lindahl

Carbon Monoxide Dehydrogenase (CODH), also known as Acetyl-CoA synthase (ACS), is one of seven known Ni containing enzymes. CODH/ACS is a bifunctional enzyme which oxidizes CO to CO_2 reversibly and synthesizes acetyl-CoA. Recently, X-ray crystal structures of homodimeric CODH from *Rhodospirillum rubrum* ($CODH_{Rr}$) and CODH from *Carboxydothermus hydrogenoformans* ($CODH_{Ch}$) have been published. These two enzymes catalyze only the reversible oxidation of CO to CO_2 and have a protein sequence homologous to that of the β subunit of heterotetrameric $\alpha_2\beta_2$ enzyme from *Moorella thermoacetica* ($CODH_{Mt}$), formerly *Clostridium thermoaceticum*. Neither $CODH_{Rr}$ nor $CODH_{Ch}$ contain an α-subunit as is found in $CODH_{Mt}$. The precise structure of the active site for acetyl-CoA synthase, called the A-cluster, is not known. Therefore, crystallization of the α subunit is required to solve the remaining structural features of CODH/ACS. Obtaining crystals and determining the X-ray crystal structure is a high-risk endeavor, and a second project was pursued involving the preparation, expression and analysis of various site-directed mutants of $CODH_{Mt.}$ Mutational analysis of particular histidine residues and various other conserved residues of CODH from

Moorella thermoacetica is discussed. Visual inspection of the crystal structure of $CODH_{Rr}$ and $CODH_{Ch}$, along with sequence alignments, indicates that there may be separate pathways for proton and electron transfer during catalysis. Mutants of a proposed proton transfer pathway were characterized. Four semi-conserved histidine residues were individually mutated to alanine. Two ($His116_{Mt}$ and $His122_{Mt}$) were essential to catalysis, while the other two ($His113_{Mt}$ and $His119_{Mt}$) attenuated catalysis but were not essential. Significant activity was "rescued" by a double mutant where His116 was replaced by Ala and His was also introduced at position 115. Activity was also rescued in double mutants where His122 was replaced by Ala and His was simultaneously introduced at either position 121 or 123. Activity was also "rescued" by replacing His with Cys at position 116. Mutation of conserved Lys587 near the C-cluster attenuated activity but did not eliminate it. Activity was virtually abolished in a double mutant where Lys587 and His113 were both changed to Ala. Mutations of conserved Asn284 also attenuated activity. These effects suggest the presence of a *network* of amino acid residues responsible for proton transfer rather than a single linear pathway.

ACKNOWLEDGMENTS

I would like to express my heartfelt gratitude to my research advisor, Professor Paul A. Lindahl, for his guidance, supervision and support during the course of my graduate program. I would like to thank Professor Marcetta Y. Darensbourg, Professor Frank M. Raushel, and Professor James C. Sacchettini for serving as my advisory committee.

I would also like to thank my past and present co-workers in Dr. Lindahl's research group who all, at one point or another, contributed to my scientific education by teaching me how to ask the right questions and to my life by their friendship. I express my thanks to Dr. Huay-Keng Loke, Dr. Xangshi Tan, Mattew Bramlett, Jian Feng, Brandon Hudder, Dr. Ivan Surovtsev, Sandy Lester and many others that I have enjoyed working with. I wish all of them the best of luck in their future endeavors.

In addition, special thanks are due to Dr. Juan C. Fontecilla-Camps's group for their cooperation on the crystallization project, to Mattew Bramlett of Lindahl's group for running the EPR samples, and to Mack Kuo of Sacchettini's group for his help to diffract crystals. Special thanks go to Dr. Lisa M. Perez for kindly generating the stereo image using Insight II 2000.

The value of family and friends in supporting me throughout graduate program has been immeasurable. I thank my family, friends and my husband Daewon Cho, for more love, companionship and support than I ever had asked for or could have hoped for; they have my eternal gratitude and love.

TABLE OF CONTENTS

CHAPTER Page

LIST OF TABLES

LIST OF FIGURES

ABBREVIATIONS

ACS, acetyl-CoA synthase

ACS_{Mt}, acetyl-CoA synthase from *Moorella thermoacetica*, also called carbon monoxide

Dehydrogenase ($CODH_{Mt}$)

A_o, open form of the A-cluster

A_c, closed form of the A-cluster

Bp, base pair(s)

CH_3-Co^{3+}FeSP, the methylated corrinoid iron-sulfur protein

$C_{int,}$ state of the C-cluster that is one electron more reduced than C_{red1}

CoA, Coenzyme A

CODH, carbon monoxide dehydrogenase

$CODH_{Rr}$, carbon monoxide dehydrogenase from *Rhodospirillum rubrum*

$CODH_{Ch}$ carbon monoxide dehydrogenase from *Carboxydothermus hydrogenoformans*

CoFeSP or CP, corrinoid iron-sulfur protein

C_{red1}, the one-electron reduced state of the C-cluster

C_{red2}, the three-electron reduced state of the C-cluster

$C_{ox,}$ the oxidized state of the C-cluster

DD-H_2O, distilled-deionized water

DNA, deoxyribonucleic acid

DTT, DL-dithiothreitol

EPR, electron paramagnetic resonance spectroscopy

IPTG, isopropyl-thiogalactosidase

KDa, kilodalton

LN_2, liquid nitrogen

MES, 2-(N-Morpholino)ethanesulfonic acid

MV, methyl viologen

Ni_d, the distal Ni ion

NiFeC, the nickel-iron-carbon EPR signal

Ni_p, the proximal Ni ion

OD600, absorbance at 600nm

PAGE, polyacrylamide gel electrophoresis

SDS, sodium dodecyl sulfate

SDS-PAGE, sodium dodecyl sulfate polyacrylamide gel electrophoresis

Tris-HCl, tris(hydroxymethyl)aminomethane-HCl

CHAPTER I

INTRODUCTION

Among the less common transition metal ions to be found in living systems is nickel. Currently just seven Ni-containing enzymes are known, including NiFe hydrogenases, ureases, glyoxalase I, *cis* - *trans* isomerase, Ni-containing superoxide dismutase, methyl -coenzyme M reductase, and Ni-containing carbon monoxide dehydrogenases (*1-3*). There are also a number of Ni-containing transport and assembly proteins, including the dedicated nickel uptake system NikA and Ni–specific metallochaperones such as HypA, HypB, CooJ, and UreE (*4-6*). Nickel may also be essential for mammals. Chickens and rats raised on nickel-deficient diets have liver problems (*7, 8*). Nickel deficiency affects sperm physiology in rats, and nickel ion is an effective inhibitor of the desensitized butyrylcholinesterase from human serum (*7, 8*).

The roles of Ni in the catalytic mechanisms of these enzymes are diverse. In Ni-containing hydrogenases, the Ni appears to be redox active and involved in substrate binding. These enzymes catalyze the reversible oxidation of H_2 to protons

$$H_2 \rightleftharpoons 2H^+ + 2e^- \qquad (1)$$

This thesis follows the format and style in *Biochemistry*.

The active site consists of a heterobimetallic $(S_{cys})_2Ni(\mu\text{-}X)Fe(CO)(CN)_2$ (X= O or OH) cluster (*9-15*), as shown in Figure 1. The bridging ligand X was proposed to be an oxide, or hydroxide in the oxidized state and was missing in the reduced state. Two cyanide and one carbonyl ligands ligate the iron center. The enzyme from *Desulfovibrio gigas,* which is the most widely studied, has an αβ heterodimeric structure of 89 kDa with one nickel and twelve iron ions. The metals are divided into one NiFe active site, one Fe_3S_4 cluster and two Fe_4S_4 clusters. The α subunit is 28 kDa and contains FeS clusters. The β subunit is 60 kDa and contains the NiFe active site (*16*). The Fe_3S_4 cluster is located in between two Fe_4S_4. However, the distances between two of these are slightly different; one is 5.7 Å and the other is 5.2 Å. (*10-13*).

The nickel site has been proposed to be redox active and alternate between Ni(III) and Ni(II) during catalysis. The Fe(II) site apparently remains redox inactive. The NiFe active site has four stable redox states including Ni-AB, Ni-SI, Ni-C, and Ni-R. Inactive enzyme purified in air can be activated after incubation with Hydrogen.

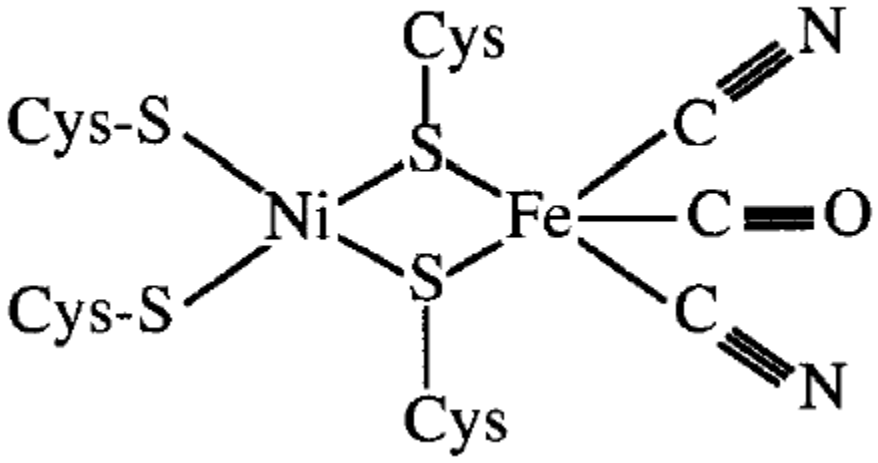

Figure 1: The active site of Hydrogenase. (adapted with permission from (*3*))

The Ni ions in ureases appear to be redox inactive and to serve as Lewis acids to stabilize certain intermediates during catalysis. Ni-containing ureases have been isolated from various bacteria, fungi, and higher plants. (*14, 17-20*). The enzyme catalyzes the hydrolysis of urea to ammonia and carbamate as shown in equation (2) (*20, 21*). The carbamate hydrolyzes spontaneously to form carbonic acid and a second molecule of ammonia in equation (3).

$$NH_2C(O)NH_2 + H_2O \rightleftharpoons H_2NC(O)OH + NH_3 \quad (2)$$

$$H_2NC(O)OH + H_2O \rightleftharpoons NH_3 + H_2CO_3 \quad (3)$$

The active site of the enzyme from *K. Aerogenes* is shown in Figure 2 (*22*). The dinickel center is bridged with a carbamylated Lys, which is a unique bridging ligand. One Ni has a coordination geometry between square pyramidal and trigonal bipyramidal, including one H_2O, two histidine ligands, one aspartate, and an oxide of the bridging carbamylated lysine. The other Ni has a trigonal planar geometry with two histidine and a bridging oxide from carbamylated lysine (*23*). Urea binds to the tri–coordinate Ni, which is followed by nucleophilic attack by hydroxide that is bound to the pentacoordinate Ni. In this enzyme, the Ni ions are thought to function in two different ways. One Ni serves as the substrate - binding site while the other is a Lewis Acid that lowers the pK of bound water.

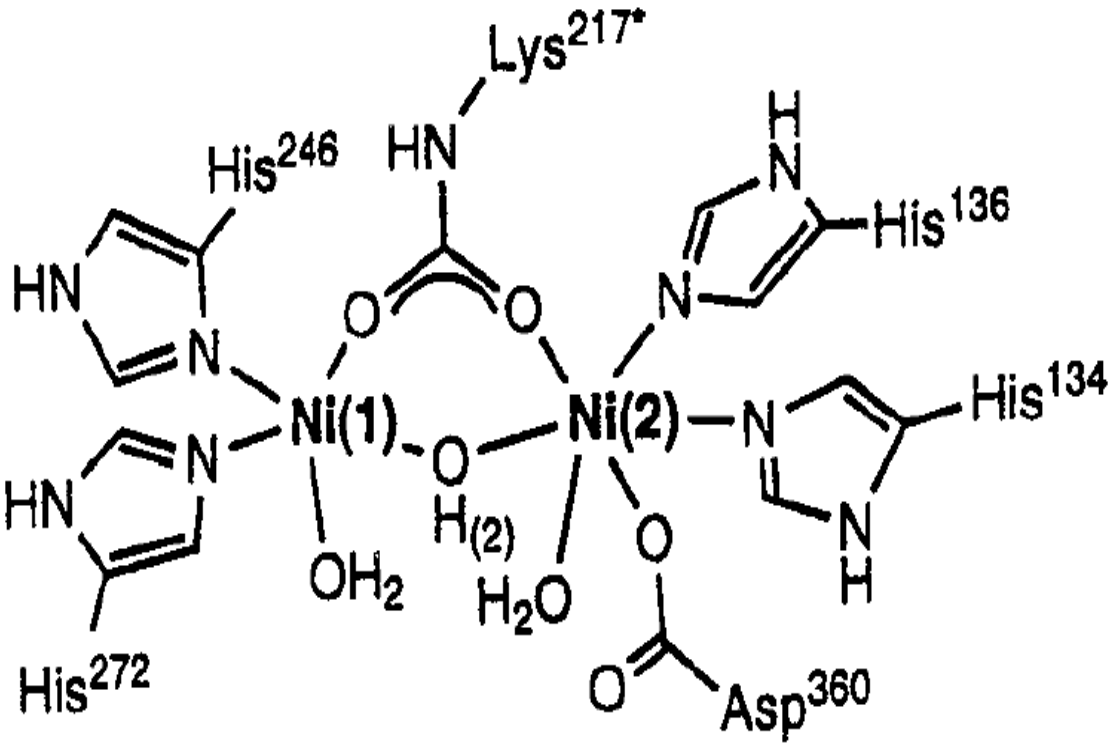

Figure 2: The active site of Urease from *K. Aerogenes*. (Adapted with permission from (*22*))

The Ni in methyl-CoM reductase appears to facilitate radical-based chemistry during the catalytic mechanism. The enzyme catalyzes the final step of methane formation, with reduction of methyl coenzyme M to methane and the heterodisulfide of CoM (which is 2-mercaptoethane-sulfonate) shown in equation (4).

$$CH_3\text{-S- CoM} + \text{H-S-CoB} \rightleftharpoons \text{CoM-S-S-CoB} + CH_4 \quad (4)$$

The enzyme is found in methanogenic archaea that are grown anaerobically. The X-ray crystallographic studies of the enzyme isolated from *Methanobacterium thermoautotrophicum* revealed the active site at 1.45 Å resolution from the inactive enzyme (*24, 25*). Methyl-CoM Reductase from *Methanobacterium thermoautotrophicum* is 300 kDa with an $\alpha_2\beta_2\gamma_2$ hexamer structure containing two molecules of the nickel porphinoid (nickel in a tetrapyrrolic structure) called coenzyme F_{430}. The active site of Methyl-CoM Reductase from *Methanobacterium thermoautotrophicum* is shown in Figure 3 (*3*). Enzyme activation occurs when the Ni(II) oxidation state in the active site is reduced to Ni(I) (*3, 26*). The Ni in the porphinoid ring is a good catalyst for methyl group reduction. Also Ni is thought to function by retention of stereoconfiguration (*26*).

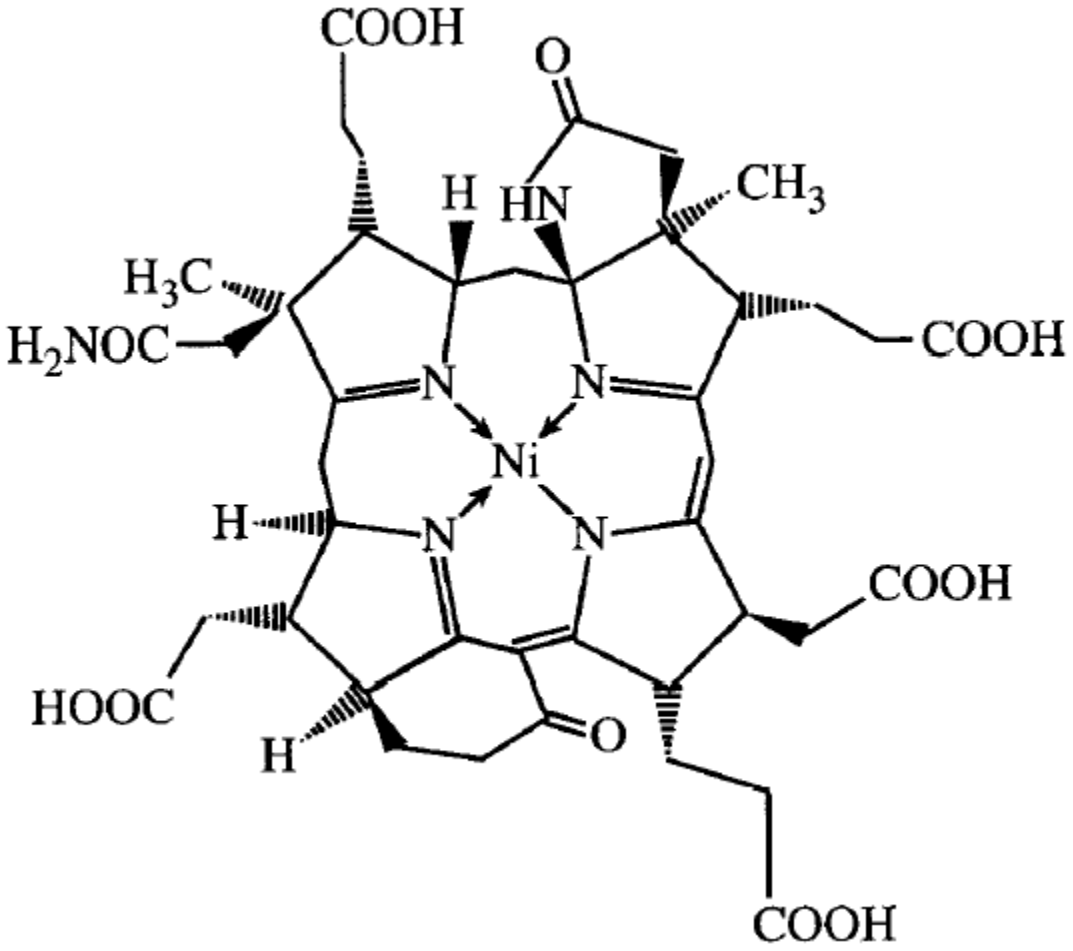

Figure 3: The active site of Methyl-CoM Reductase. Structure of coenzyme F_{430}. (Adapted with permission from (*3*))

Carbon Monoxide Dehydrogenase

For more than a quarter century, Ni-containing Carbon Monoxide Dehydrogenase (CODH) has been studied. Carbon Monoxide Dehydrogenase is found in 2 classes of Methanogenic Archaea (Class I and II), in Acetogenic Bacteria (Class III), and in CO-utilizing Bacteria (Class IV) (*27*). This enzyme has been named according to its functions. The monofunctional CODH enzyme carries out the reversible oxidation of CO. It is found in many species, for example phototrophic anaerobes such as *Rhodospirillum rubrum*. The bifunctional CODH/ACS enzyme, found in species such as the acetogenic bacterium *Moorella thermoacetica*, has a subunit homologous to the monofuctional enzymes and another subunit that is involved in acetyl Co-A synthesis. CODH/ACS enzymes are involved in the Wood/Ljungdahl carbon-fixation pathway (*27, 28*).

CODH enzymes catalyze the reversible oxidation of CO to CO_2 and the synthesis of acetyl-CoA, as shown in equations (5) and (6) (*1*).

$$CO + H_2O \rightleftharpoons CO_2 + 2H^+ + 2\,e^- \qquad (5)$$

$$CH_3Co_3{}^+FeSP + CoAS^- + CO \dashrightarrow CH_3COSCoA + Co^+FeSP \qquad (6)$$

The enzyme from *M. thermoacetica* is extremely sensitive to oxygen and contains iron-sulfur metalloclusters. Iron-sulfur clusters are assumed to be the earliest cofactors occurring in nature (*28*). Structural features of these metalloclusters have been

determined by spectroscopic and biochemical studies (*1, 29-33*). However, it is very difficult to answer structural questions without an X-ray diffraction structure.

$CODH_{Mt}$ has an $\alpha_2\beta_2$ quaternary structure of 310 kDa containing four metallocenters, the A, B, C and D clusters. The α subunit contains the A-cluster while the β subunit contains the B, C, and D clusters. Both A and C clusters are novel Ni-Fe-S clusters (*31- 33*). The A-cluster is the active site for the synthesis of acetyl-CoA from CO, CoA, and a methyl group donated from a corrinoid-iron-sulfur protein (CoFeSP). The C-cluster catalyzes CO to CO_2 oxidation reversibly (*1, 33*). The B and D clusters are $[Fe_4S_4]^{2+/1+}$ cubes involved in electron transfer reactions (*29, 34, 35*). Carboxydotrophic bacteria, such as *Rhodosprillium rubrum* (Rr) and *Carboxythermus hydrogenoformans* (Ch), consist of only the β subunit (*35, 36*). The D cluster bridges the two β subunits.

Research Objective

$CODH/ACS_{Mt}$ has been studied in our lab for the last fifteen years. To solve the structural features and mechanisms of the enzyme, spectroscopic and kinetic studies were done. My objective was to investigate the crystallization of $CODH/ACS_{Mt}$ and the α subunit of $CODH/ACS_{Mt}$. Obtaining crystals and determining the X-ray crystal structure is a high-risk endeavor, and so we pursued a second subsidiary project involving the preparation, expression and analysis of various site-directed mutants of $CODH_{Mt.}$

CHAPTER II

CRYSTALLIZATION STUDIES OF CODH FROM *MOORELLA THERMOACETICA* *

Background

X-ray crystal structures of the homodimeric CODH from *Rhodospirillum rubrum* (with 2.8 Å resolution) and CODH from *Carboxydothermus hydrogenoformans* (with 1.6 Å resolution, shown in figure (1)) have been published (*35, 36*). These two enzymes catalyze only the reversible oxidation of CO to CO_2 and have protein sequence homologous to that of the β subunit of CODH from *Moorella thermoacetica* ($CODH/ACS_{Mt}$). Neither enzyme contains an α-subunit like that found in $CODH/ACS_{Mt}$. The structure of the A-cluster was proposed to be a mononuclear Ni site bridged through an unidentified molecule to a 4Fe-4S cube (*31*).

An X-ray crystal structure of CODH/ACS from *Moorella thermoacetica* (with 2.2 Å resolution, shown in figure 4B) has been reported (*37*). The A-clusters of this structure contain a 4Fe-4S cube bridged to a binuclear site which contains one Cu and one Ni. The presence of Cu was unexpected. Doukov *et al*. suggested that the Cu was essential for

* Part of this chapter is reprinted with permission from "Ni-Zn-[Fe4-S4] and Ni-Ni-[Fe4-S4] clusters in closed and open αsubunits of acetyl-CoA synthase/carbon monoxide Dehydrogenase" Darnault C., Volbeda A., Kim, E. J. , Legrand, P., Vernede, X., Lindahl, P. A. and Fontecilla – Camps, J. C. (2003) *Nature Struct. Biol.* **10**, 271 – 279. copyright 2003 by Nature publishing group.

catalysis. However, the Cu-based structure could not explain the known heterogeneity of the cluster because only a single type of Ni is observed.

Recently, the genes encoding CODH/ACS_{Mt} (ACS_{Mt} αβ) have been cloned and expressed in *E. coli,* affording active enzyme that is virtually indistinguishable from that synthesized in *Moorella thermoacetica* (*38*). After adding Ni, the α subunit of ACS_{Mt} isolated from *E. coli* contains an intact A-cluster (*39*). Populations of α subunits are heterogeneous. About 30-50% of theses subunits have Ni-labile ACS and the other have nonlabile ACS. Only labile-Ni portion of ACS_{Mt} αβ exhibits catalytic activity and the NiFeC EPR signal. The A-cluster lacking Ni ions can be reconstituted by incubation with $NiCl_2$ (*40*). After activation with $NiCl_2$, the α -subunit has an EPR spectrum identical to that of ACS_{Mt} αβ and it exhibits acetyl-CoA synthase activity (*38, 39*). This capability allows site – directed mutants of the α subunit to be prepared.

Objective

One objective of this project was to obtain crystals and solve the X-ray crystal structure of the α subunit and possibly the entire enzyme (CODH/ACS). Another objective was to elucidate structural features of the enzyme relevant to the catalyst mechanism.

A

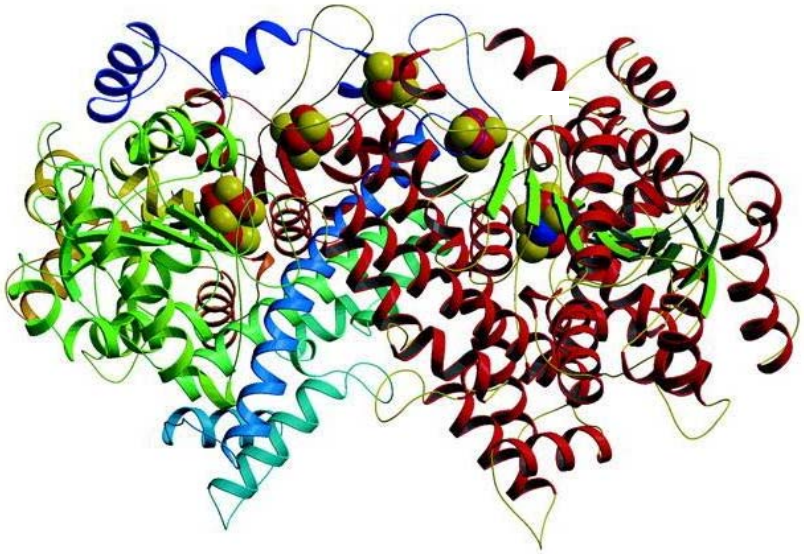

B

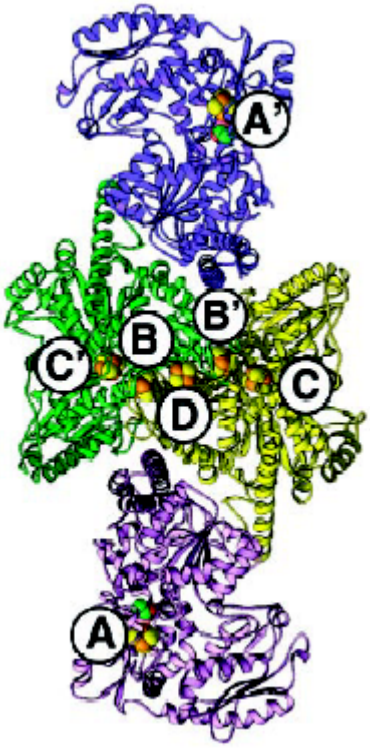

Figure 4: Published structures of $CODH_{Ch}$ and $CODH/ACS_{Mt}$. A: the CODH II dimer of *Carboxydothermus hydrogenoformans.* (Adapted with permission from *35*), B: Structure of CODH/ACS from *M. thermoacetica* (Adapted with permission from*37*).

Crystallization Methods

150 years ago, the first protein hemoglobin was crystallized (*41*). Since then, the structure of about 8000 proteins and nucleic acids, and 1300 macromolecules have been determined (*42*). To analyze a protein structure, we need to obtain a suitable single crystal. To get a single crystal, there are some general requirements such as purity of enzyme, solubility, pH, temperature, etc. Alexander McPherson, at the University of California, Irvine, suggested 10 practical principles, which can be applied, whatever the molecule. The 10 principles are homogeneity, solubility, stability, super- saturation, association, nucleation, variety, control, impurity, and preservation (*41, 42*). However, every crystallographer has his or her own opinion and know-how. First of all, the enzyme needs to be reasonably pure, generally greater than 95%. Usually, greater purity results in better crystals. But sometimes, extreme purity can be a bad thing because it hampers nucleation. When the desired purity of the protein is achieved, crystallization trials need to be set up using different crystallization methods. The most popular crystallization method is the vapor diffusion method. The vapor diffusion method may be subdivided into several techniques including, hanging drop, sitting drop, sandwich drop, reverse vapor diffusion, and pH gradient vapor diffusion (*41-43*). In addition, there are different methods of crystallization, for example, the batch method, dialysis, temperature-induced, free interface diffusion, seeding, and bulk crystallization (*43*). Crystallization of a protein can be affected by variable parameters, such as protein concentration, pH, nature and concentration of precipitant, buffer, temperature, and salt (*41, 42, 44*). To find out the conditions for crystallization of the protein, we need to

make different conditions of screening solution. In 1991, sparse matrix sampling was developed by Jancarik and Kim (*44*). Solutions based on this screening approach are available commercially from Hampton Research and elsewhere. Although crystallization is a trial-and-error procedure, the obtained conditions after initial screening can be designed by a factorial approach, which involves constructing a table with changing variable parameters. This step is called adjusted screening. The final step would be optimized screening with condition obtained from the adjusted screening step. This is the most popular method for crystallization. Early protein crystallographers tried to measure dried crystals, but they did not show X-ray diffraction patterns, so J. D. Bernal and Dorothy Crowfoot exposed the crystal with mother liquor in 1934, and observed that they could get sharp diffraction patterns (*42*). However, the mother liquor contains water molecules, which make ice-crystals. The Cryocooling method was developed by Garman and Schneider in 1997. Cryoprotectants, which contain antifreeze, are used to prevent ice formation in and around the crystal.

Materials and Methods

Bacterial growth and harvesting as well as protein purification and characterization were performed as described (*40, 45-47*). The α subunit in different forms were prepared and crystallized, including the oxidized, reduced, CoA bound, methylated and CO-bound forms. Mutants of the α subunit were also prepared and crystallized.

Hanging Drop Vapor Diffusion Method

. The hanging drop vapor diffusion method was used for crystallization studies. This is the most popular crystallization method. The difference in concentration between the reservoir and the drop drives the closed system to equilibrium by diffusion through the vapor phase.

The hanging drop method is easy to perform and needs only a small amount of protein. Other advantages include an ability to view the drop through a glass cover slip, easy access to the drop, and a reduced chance that the crystal will stick on the wall of the plastic tray (*41, 42, 44*).

From these trials, any micro-crystals obtained were used as seeds for growing larger crystals. The final step, called optimized screening, used conditions obtained from the adjusted screening step.

Mounting the Crystals

For mounting the crystals with cryoloops, liquid nitrogen (b.p. –196 °C) was brought into the glove box in a cold room to freeze the crystals. The process of mounting the crystal for data collection is as follows: 1. Adjust the size of cryoloop to the size of the crystal. 2. Flip down the cover slip, mounting the crystal with the cryoloop under a microscope. 3. Dip the crystal into the cryoprotectant to wash off water. 4. Immediately freeze the mounted crystal in the liquid nitrogen. 5. Store it in a vial with liquid nitrogen. Using this protocol, the samples were sent to our collaborator, Professor Juan C. Fontecilla-Camps at the *Laboratoire de Cristallographie et Cristallogense des Proteinès*, of *institut de biolologie structurale* in Grenoble, France. X-ray diffraction data were collected and analyzed at the *CEA/CNRS* facility in Grenoble, France. Appropriate single crystals were analyzed via X-ray diffraction. Synchrotron radiation was used to collect higher resolution data. The cryocooling method was used for mounting of the crystals and collecting of the data.

Results and Discussion

CODH was purified and characterized from *Moorella thermoacetica* as described (*40, 45-47*). Recombinant α -subunit was expressed in *E. coli* and purified (*38, 39*). Crystallization of proteins can be affected by various parameters, such as protein concentration, pH, the nature and concentration of precipitant, buffer, temperature, and salt, and so many of these parameters were varied (*41, 42, 44*). Using the hanging drop method, fast screening was performed initially. A screen kit from Hampton Research was then used for an adjusted screening step.

Crystals were grown at ~ 4 °C in an anaerobic glove box. In the past two years, over 200 trays (24 hanging drops per tray) were prepared and screened. Five different forms of crystals were obtained (4 are shown in Figure 5) including a) a cube-type crystals, b) a needle-type crystal, c) pentagonal or hexagonal crystals, d) cubic micro-crystals (not shown), and e) a rectangular crystal superimposed by a fiber or hair-like material. Pentagonal or hexagonal shape crystals were obtained with sharp edges after 4 days, but over time, as evident from the picture, the sharp edges became dull.

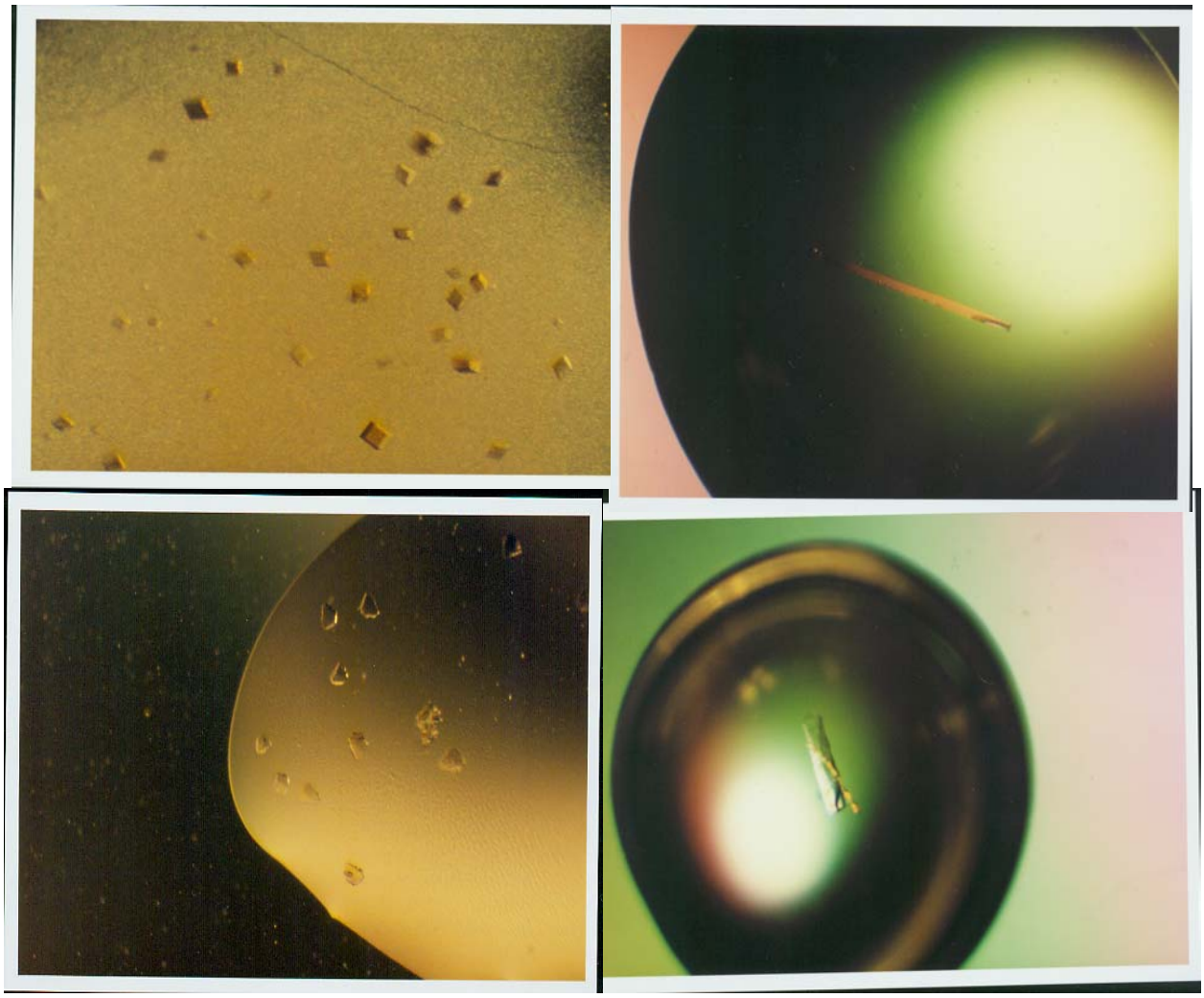

Figure 5: Crystals obtained at ~ 4 °C. Top left - Cube, Top right - Needle, Bottom left - Pentagon or hexagon, Bottom right - Rectangular.

Cube-type crystals were obtained from 1.5 M Li_2SO_4 and pH 7.5 Hepes-Na after 5 months with a 32 mg/mL sample of the α-subunit. Micro-cube crystals formed within 4 days with low concentration of Li_2SO_4 and 30 % of PEG 4000 in pH 8.5 Tris-HCl. Needle-type crystals formed in 0.1 M sodium dihydrogen phosphate / 0.1M potassium dihydrogen phosphate, pH 6.5 MES, 2 M NaCl with 5mg/mL of enzyme. Pentagonal or hexagonal shape crystals were obtained with sharp edges after 4 days using 12 % of PEG 20000, pH 6.5 MES with ~ 5 mg/mL of α-subunit protein. The rectangular shaped crystal was produced in 0.2 M sodium chloride and 0.1 M sodium dihydrogen phosphate / 0.1 M potassium dihydrogen phosphate, pH 6.5 MES. Every trial was performed at 4 °C in an anaerobic glove box. The greatest difficulty in obtaining crystals results from the extreme oxygen sensitivity of the enzyme. All crystals must be prepared in atmosphere containing < 2 ppm of O_2. Another concern was temperature stability. The temperature of our laboratory varied by ± 8 °C over a 24-hour period. To address both problems, we built a cold room around a Vacuum/Atmosphere glove box. This allowed crystallization experiments to be performed under strict anaerobic conditions at cold and relatively stable temperature (8 ± 3 °C). However, these conditions increase the difficulty of the experiment. All plastic ware, pipette tips, and trays must be placed in the glove box one week prior to handling them. All buffers are degassed under vacuum. This procedure changed their concentrations, requiring that concentrations be redetermined using the refraction index of calibrated standard solutions. It is also difficult to mount crystals using a 0.2 - 0.3 mm diameter cryoloop under a microscope wearing thick rubber gloves.

Crystals were mounted for data collection using the cryocooling method. To prevent ice-crystalline formation, the cryoprotectant paratone-n was chosen for this study. Paratone-n produces a significant background in the X-ray diffraction pattern, but it protects the enzyme from oxygen. Cryoloops were used to mount the crystals. Liquid nitrogen (b.p. –196 °C) was brought into the glove box to freeze the crystals. Using this protocol, 8 samples were sent to Grenoble, France to collect data at the European Synchrotron Radiation Facility. The crystals diffracted at ~ 4 Å resolution.

Using the seeding method, the cube-shaped crystals were obtained quickly. However, over time they grew a little bit bigger, and the crystals obtained were twinned in which two crystals are bound in the shape of an "X". Optimal conditions still need to be identified, including a stabilizing solution, the dilution factor, the number of seeds and a different technique of adding the seed.

A 50 kDa fragment of the α subunit (with a 30 Kda domain deleted) was crystallized at 20 °C by our collaborators. The A-cluster is intact in this form, and we felt that truncating this domain would facilitate crystallization. The crystal (Figure 6) was 0.25 mm x 0.25 mm x 0.15 mm and diffracted to 4.5 Å resolution.

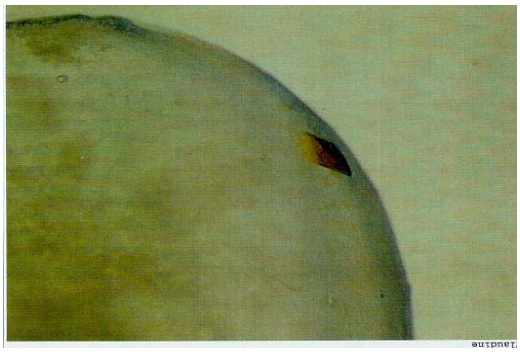

Figure 6: A crystal of a 50 kDa fragment of the α subunit.

Better crystals of CODH/ACS and CO-treated CODH were obtained by our collaborator after adding dimethylethyl ammonium propane sulfonate with my adjust condition. A monoclinic space group C2 crystal form with a ≈ 245 Å, b ≈ 82 Å, c ≈ 167 Å, β ≈ 96 ° was obtained with the hanging drop method at 20 °C. Crystallization solution was prepared containing 2 mM sodium dithionite, 10 mM DTT, 1.95-2.10 M ammonium sulfate, 100 mM HEPES at pH 7.0-7.3, 3.5 % PEG 400, and 100-200 mM dimethylethyl ammonium propane sulfonate (NDSB195). Hanging drops were prepared by 1:1 ratio with 10 mg/ml enzyme and crystallization solution.

The structure of CODH/ACS and CO-treated ACS were solved to 2.2 Å and 1.9 Å resolution, respectively. The structure of Doukov *et al*. has Cu in closed form, but our structure has two different types of A-clusters, named closed form and open form shown in figure 7. We believe our structure is active form of CODH /ACS supported by Bramlett *et al*.'s recent study (*48*).

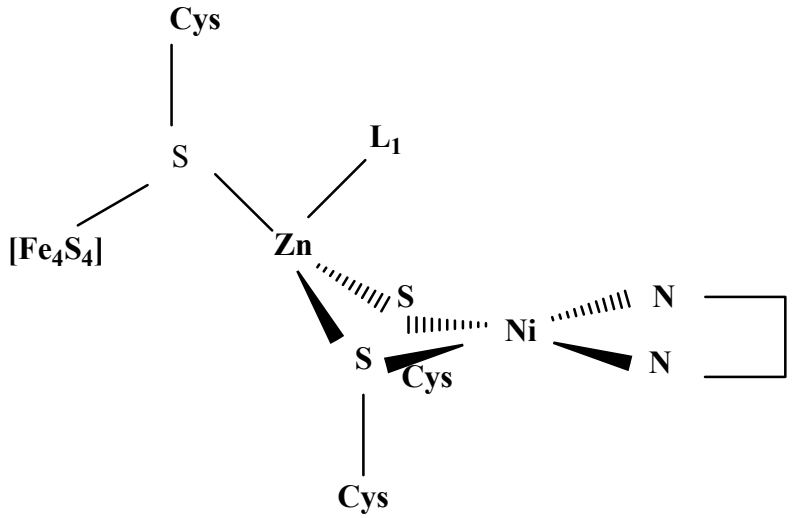

Closed Form

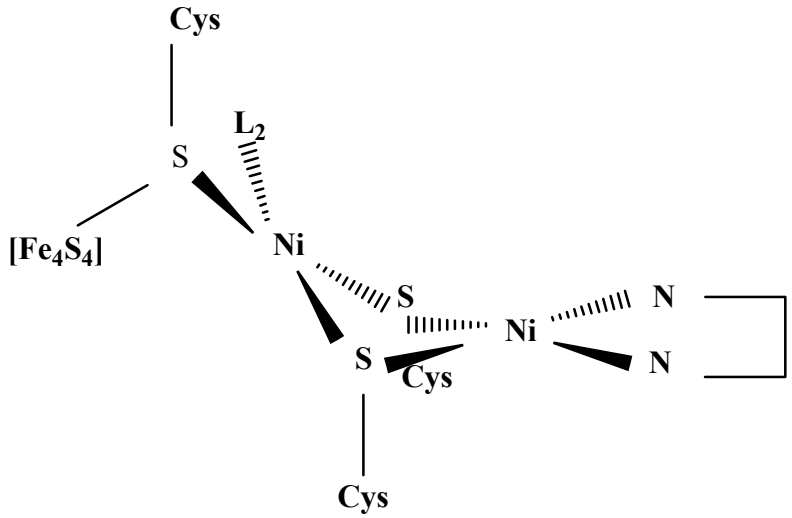

Open Form

Figure 7: The A- cluster structure of CODH/ACS from *M. thermoacetica.*

The structure of the A-cluster was proposed from EPR and Mössbauer spectroscopic investigations. The proposed A-cluster was a Ni atom bridged to a 4Fe-4S cube through an unidentified molecule (*31*). The A-cluster is methylated during catalysis, and the enzyme must be reduced for this to happen. However, the site of reduction has not been identified. This redox site, named the D-site, appeared to be a n = 2 redox center, possibly a redox-active cystine located near Ni in the A-cluster (*46*). This hypothesis was discarded by Darnault and coworkers because a pair of cysteine residues does not exist near Ni in the A-cluster (*49*). We suggested the redox site may be Ni(0) (*49*).

CHAPTER III

MUTATIONAL ANALYSIS OF PARTICULAR HISTIDINE RESIDUES AND VARIOUS OTHER CONSERVED RESIDUES OF $CODH_{Mt}$

Introduction

Ni-containing carbon monoxide dehydrogenases (CODH's) and acetyl-CoA synthases are found in methanogenic archaea, acetogenic bacteria, and CO-utilizing bacteria, where they play critical roles in C_1-metabolism (*50*). This family of enzymes catalyzes reaction [7].

$$CO + H_2O \rightleftarrows CO_2 + 2e^- + 2H^+ \qquad (7)$$

The enzymes from *Rhodospirillium rubrum* ($CODH_{Rr}$) and *Carboxydothermus hydrogenoformans* ($CODH_{Ch}$) are β_2 homodimeric, while that from *Moorella thermoacetica* ($CODH_{Mt}$) is an $\alpha_2\beta_2$ tetramer in which the β subunits are homologues to those of $CODH_{Rr}$ and $CODH_{Ch}$. $CODH_{Mt}$ is bifunctional and also catalyzes the synthesis of acetyl-CoA. This chapter focuses on reaction [7]) and acetyl-CoA synthase aspects will not be discussed.

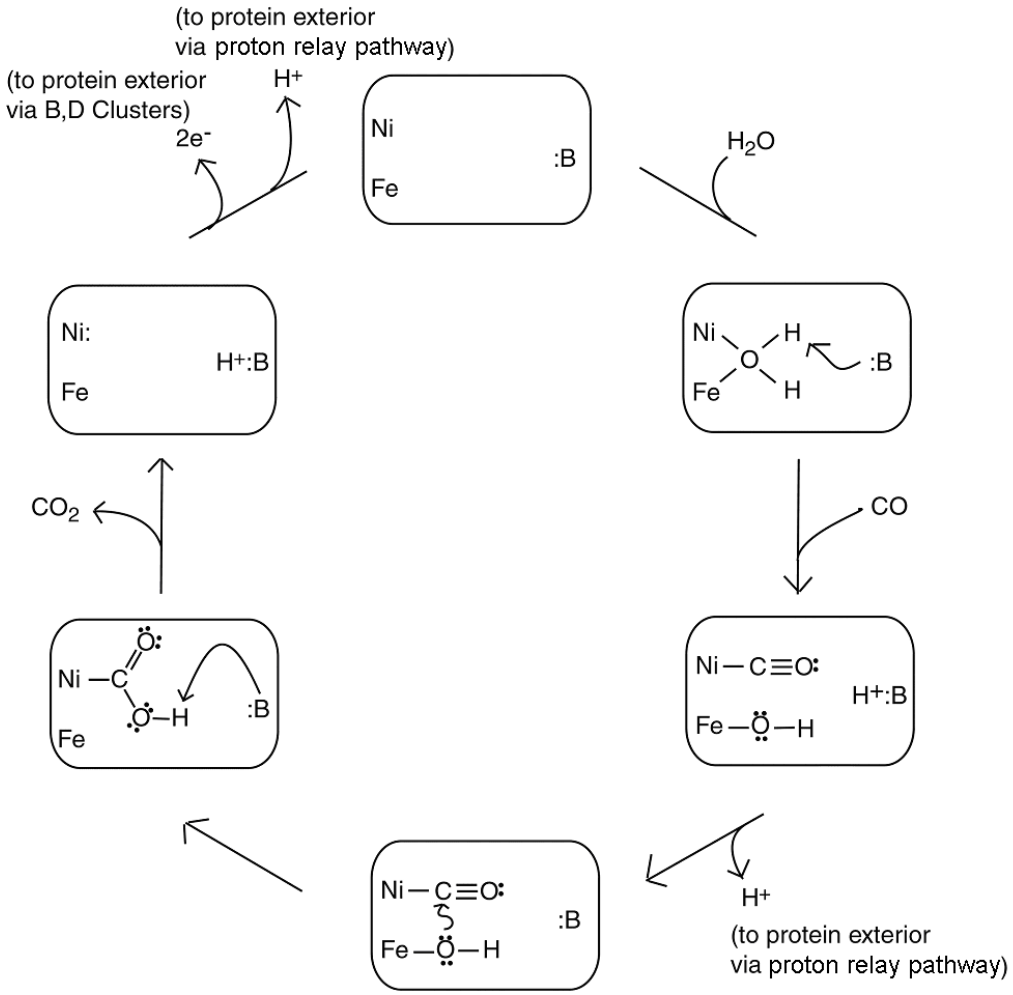

Figure 8: Mechanism of CO oxidation by CODH. Emphasizing protons and electrons transfer. Ni and Fe represent the [Ni Fe] subsite of the C-cluster while :B represents a base used in catalysis.

Four structures have been reported, including one each of $CODH_{Ch}$ and $CODH_{Rr}$, and two of $CODH_{Mt}$ (*35-37, 49*). Structures are grossly equivalent, though there are minor structural differences that may be functionally significant. The C-cluster of $CODH_{Mt}$ as reported by Darnault *et al*. is structurally heterogeneous (*49*).

During the catalytic oxidation of CO to CO_2, water probably binds in bridging fashion to the Ni and unique Fe in a redox state of the C-cluster called C_{red1} (Figure 8) (51). An unidentified base near to the C-cluster abstracts a proton from water and CO binds to the Ni. The resulting nucleophilic hydroxyl group attacks the carbon of Ni-CO, forming a Ni-bound carboxylate. Either the same or a different base abstracts the proton of this carboxylate, leading to the dissociation of CO_2 and the two-electron reduction of the cluster, thereby forming a state of the C-cluster called C_{red2}. C_{red1} and C_{red2} states exhibit characteristic EPR signals with g_{av} = 1.82 and 1.86, respectively (*52, 53*). An $[Fe_4S_4]$ *D-cluster* bridges the two β subunits and is surface-exposed while an $[Fe_4S_4]$ *B-cluster* is located within eachβ subunit roughly along a line between the C- and D-clusters, with clusters spaced ~ 12 Å apart.

Redox properties of the B- and D-clusters and their position and spacing relative to the active-site C-cluster unambiguously identifies them as constituting an electron transfer pathway between the C-cluster and redox partners external to the enzyme.

In contrast, little is known about the base(s) used to abstract protons during catalysis or about the pathway used to transfer protons between the C-cluster and the protein surface. There are ~ 4 semi-conserved histidine residues in the 18 CODH primary sequences reported (*54*), including $His113_{Mt}$ (124_{U}), $His116_{Mt}$ (127_{U}), $His119_{Mt}$ (130_{U}), and $His122_{Mt}$ (133_{U}) (Tables 1 and 2). Due to its proximity to the C-cluster, Drennan *et al*. suggested that His95 of $CODH_{Rr}$ (corresponding to His 113 of $CODH_{Mt}$) might act as a catalytic base (*36*). They noted that this residue was positioned at the top of a putative cationic tunnel lined by residues His98, His101 and His108 of $CODH_{Rr}$ (corresponding to His116, His119, and Glu126 of $CODH_{Mt}$). They also suggested that Lys568 of $CODH_{Rr}$ (corresponding to Lys587 of $CODH_{Mt}$) could stabilize a metal-bound carboxylate intermediate during catalysis.

Table 1. Sequence alignment of the containing C-Cluster subunit (*50, 54*).

ORGANISM	**RESIDUE NUMBER**		
	123----------137	297-300	724-726
M.thermoautotrophicum	A**H**AG**H**AR**H**LVD**H**LIE	IGH**N**	Q**K**A
M. jannaschii I	C**H**AG**H**SR**H**LV**HH**LIE	IGH**N**	Q**K**A
A. fulgidus I	A**H**TG**H**AR**H**ML…**H**DIE	IGH**N**	Q**K**A
M. frisia I	C**H**AA**H**GR**H**LLD**H**LIE	IGH**N**	Q**K**A
M. frisia II	C**H**AA**H**GR**H**LLD**H**LIE	IGH**N**	Q**K**A
M. thermophila	C**H**AA**H**GR**H**LLD**H**LIE	IGH**N**	Q**K**A
M. soehngenii	A**H**TA**H**GR**H**LY…**H**WCL	YGH**N**	Q**K**A
A. fulgidus II	A**H**TA**H**AR**H**LVD**H**LIE	VGH**N**	H**K**A
R. rubrum	A**H**SE**H**GR**H**IALAMQ**H**	NGH**N**	E**K**A
M. thermoacetica	A**H**CE**H**GN**H**IA**H**ALVE	HGH**N**	G**K**A
C. hydrogenoformans	G**H**SG**H**AK**H**LA**H**TLKK	HGH**N**	E**K**A
C. difficile I	A**H**SD**H**ARDIA**H**TL…A	HGH**E**	E**K**A
C. acetobutylicum I	TYS**HH**AYEAYRTLKA	NGH**Q**	Q**K**A
A. fulgidus III	AYTY**H**AIEAAKTLKA	NGH**E**	Q**K**A
C. acetobutylicum II	CYV**H**VVETTARNLKA	TGH**Q**	E**Q**A
C. difficile II	CYL**H**VVENTAKNLKN	TGH**Q**	E**Q**A
M. jannaschii II	CYV**H**CAENAARALLS	TGH**Q**	E**Q**A
M. kandleri	CYV**H**CLENAARALKS	TGH**Q**	E**Q**A

Table 2. Comparison of number system. Subscript indicates the species. (Mt: *M. thermoacetica*, Rr: *R. rubrum*, U: Universal).

M. thermoacetica	*R. rubrum*	*Universal*
$His113_{Mt}$	$His95_{Rr}$	$His124_{U}$
$His116_{Mt}$	$His98_{Rr}$	$His127_{U}$
$His119_{Mt}$	$His101_{Rr}$	$His130_{U}$
$His122_{Mt}$	-	$His133_{U}$
$Glu126_{Mt}$	$His108_{Rr}$	
$Ala121_{Mt}$	-	$Ala132_{U}$
$Ala123_{Mt}$	-	$Ala134_{U}$
$Glu115_{Mt}$	-	$Glu126_{U}$
$Gly117_{Mt}$	-	$Gly128_{U}$
$Lys587_{Mt}$	$Lys568_{Rr}$	$Lys725_{U}$
$Asn284_{Mt}$	$Asn266_{Rr}$	$Asn300_{U}$

Objective and Approach

The objective of this project is to determine whether the four conserved histidines function as a proton relay during catalysis. Our approach was to perform site-directed mutagenesis of the histidine residues and then perform enzyme activity assays, and EPR spectroscopy to determine whether they are involved in proton transfer. If these residues are part of a proton-relay, the pK_a's of their imidazole side-chains may affect the overall activity versus pH profile. If any or all of these residues are changed to alanine, activity should be severely attenuated, possibly in proportion to the number of histidine mutated. Thus, we would make single, double, triple and quadruple alanine mutants. We would attempt to "rescue" activity by adding imidazole, which is the ionizable group of histidine, to assay solutions. We would also mutate one or more of these histidines (pK_a = 6.03) to cysteine (pK_a = 8.07) and aspartic acid (pK_a = 3.90). If proton transfer requires a free base, the pH profile of these mutants might be substantially different from wild-type $CODH_{Ct}$. The cysteine mutant might be active only at high pH, while the aspartic acid mutant might be active at any pH above 4-5 (but might not show reversible catalysis). We would make mutations of neighbor residues to recover mutants of essential His residues and mutants of alternative conserved residues based on the crystal structures.

Materials and Methods

Construction of Mutants

Oligonucleotides used to construct mutants were synthesized in the Gene Technologies Laboratory at Texas A&M University. Mutants were constructed using the QuikChange site-directed mutagenesis method from Stratagene, using plasmid pTM02, which contains the genes *acsA* and *acsB*, as the template (*38*). Double mutants were constructed using one oligonucleotide containing both mutations. All mutant plasmids were produced using an MJ Research Minicycler PCR machine.

Proteins Characterization

Mutants were transformed, expressed, harvested, and purified as described (*38*). Protein concentrations were determined by the Biuret method (*55*). Standard CO oxidation activity assays at pH 8 were performed as described (*40*). Other assays were performed identically except at pH 5 (in sodium acetate buffer), pH 6 (in MES), pH 7 and 9 (in Tris - HCl). Mutants His113Ala and His116Ala were incubated with 50 mM imidazole (final concentration) for 1 hr and then assayed for activity in standard assay buffer. EPR measurements were recorded on a Bruker EMX spectrometer as described (*38*).

Results

Proton Transfer Mutants

The mutant $CODH_{Mt}$ proteins listed in Table 3 were constructed and isolated as described in *Materials and Methods*. In each case, purity was > 80% and the recombinant proteins were soluble in standard buffers. Proteins were brown, indicating the presence of Fe-S clusters. Mutant proteins His113Ala:His122Ala, His116Ala, Glu115His:His116Ala, His119Ala, His122Ala:Ala123His, Lys587Ala, and Asn284Ala exhibited the well-characterized EPR signals from B/D- and C-clusters (Figure 9). The high yields, solubility, color, and EPR spectra indicate that these mutant proteins were properly folded and had the standard set of metal centers found in the wild-type enzyme.

CO oxidation activities for each mutant were obtained in solutions buffered at various pH values (Figure 10 and Table 3), except for $Lys587Ala_{Mt}$ whose activity was determined only at pH 8. Activities generally increased as pH increased, consistent with the thermodynamic influence of generating protons as products of reaction [7]. Deleting each of the four semi-conserved His residues had different effects on activity. Activity was nearly abolished in the two mutant proteins where Ala replaced $His116_{Mt}$ and $His122_{Mt.}$ In contrast, activity was attenuated relative to WT but still significant in mutants where Ala replaced $His113_{Mt}$ and $His119_{Mt}$. This latter behavior suggests that

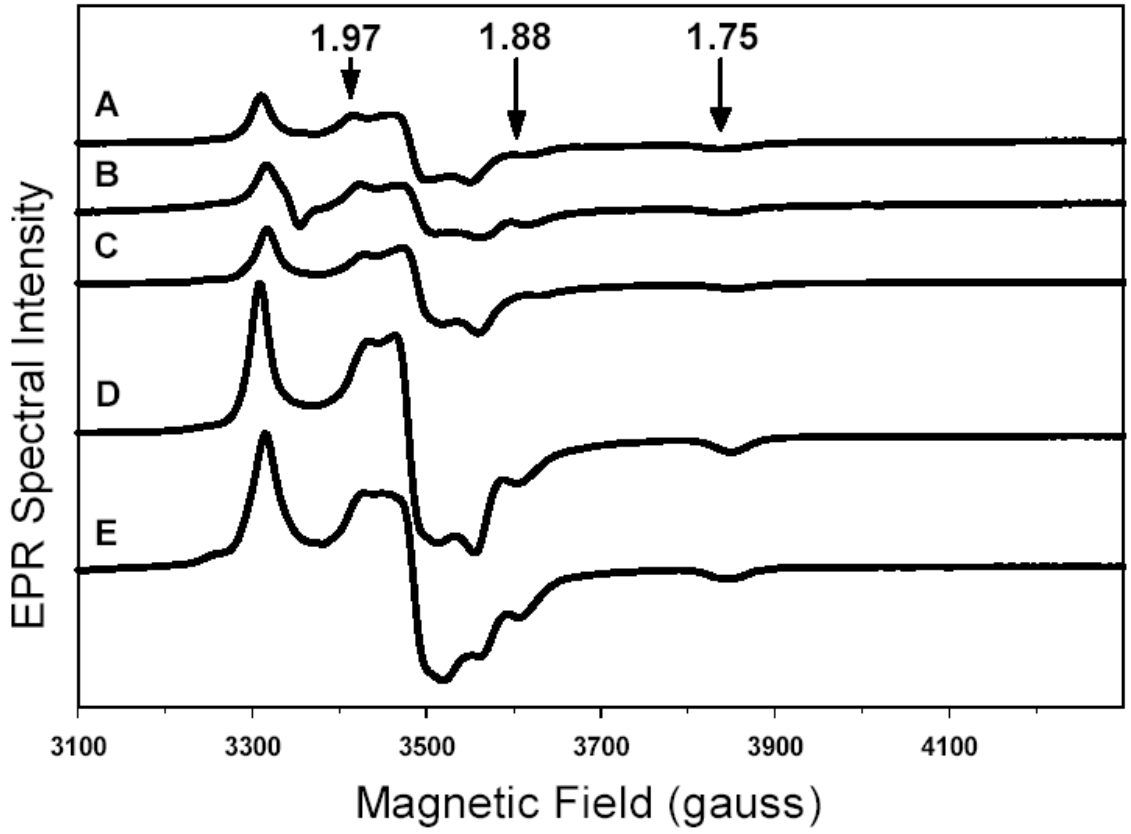

Figure 9: EPR spectra of mutants used to identify a proton pathway in CODH $_{Mt}$. A) His113Ala$_{Mt}$ (His124Ala$_{U}$) – His122Ala$_{Mt}$ (His133Ala$_{U}$), B) His116Ala$_{Mt}$ (His127Ala$_{U}$), C) His119Ala$_{Mt}$ (His130Ala$_{U}$), D) Asn284Ala$_{Mt}$ (Asn300Ala$_{U}$), E) Lys587Ala$_{Mt}$ (Lys725Ala$_{U}$). Arrows from left to right indicate the gav = 1.86 signal from the Cred2 state of the C-cluster. X-band EPR of CODH$_{Mt}$ at 10K was essentially performed as described (*38*).

these residues are involved in catalysis, but may serve redundant functions with other groups. The relative activity of the double-mutant with both of these residues replaced with Ala (i.e. $His113Ala_{Mt}$:$His119Ala_{Mt}$) was close to the *product* of the relative activities of the individual mutants ($44\% \times 27\% = 12\% \approx 15\%$ as observed). Activities of Lys587Ala and Asn284Ala mutants were significant but attenuated relative to WT.

Activity was not "rescued" by incubating His116Ala or His113Ala in buffer containing imidizole. However, double-mutants Glu115His:His116Ala, His122Ala:Ala123His and Ala121His:His122Ala did exhibit significant activity (Table 3). These endogenous "rescue" experiments suggest that the function(s) of His116 and His122 do not depend on their *exact* location. The substantial recovery of activity with double mutant His122Ala:Ala123His is congruent with the fact that some CODH's have a conserved His residue at position 123 instead of 122 (Table 1). Mutant His116Cys also exhibited substantial activity, indicating that Cys can partially mimic the function of His. Like His, Cys has an ionizable hydrogen in its R group and can serve as a general base. Our colleague, Matt Bramlett checked activity of $K587A_{Mt}$ mutant, which has 42 % activity relative to wild type.

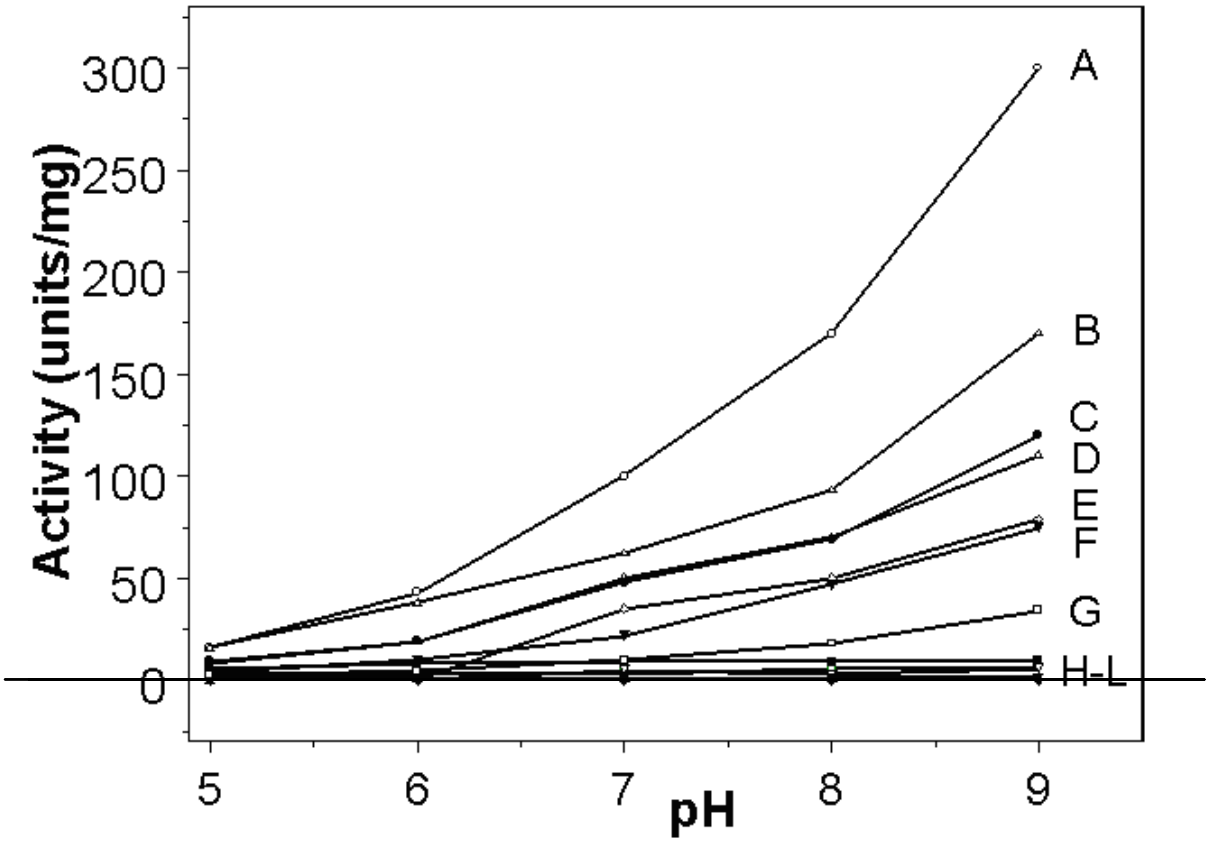

Figure 10: CO oxidation activity vs. pH for WT $CODH_{Mt}$ and various mutants. Activities of mutants were checked as described in experimental procedure. A) wild-type, B) $His122Ala_{Mt}$:$Ala123His_{Mt}$, C) $His116Cys_{Mt}$, D) $His113Ala_{Mt}$, E) $His119Ala_{Mt}$, F) $Glu115His_{Mt}$:$His116Ala_{Mt}$, G) $Ala121His_{Mt}$:$His122Ala_{Mt}$, H) $His113Ala_{Mt}$:$His119Ala_{Mt}$, I) $His116Ala_{Mt}$, J) $His122Ala_{Mt}$, K) $His116Ala_{Mt}$:$Gly117His_{Mt}$, L) $His116Asp_{Mt}$, m: $His113Ala_{Mt}$:$His116Ala_{Mt}$:$His119Ala_{Mt}$.

Table 3. CO Oxidation activities of $CODH_{Mt}$ mutant proteins. Activities were determined as described in Materials and Methods. Three different and independent wild-types preparations were used as controls for calculating the percentage activities of His,Cys, Asn and Lys Mutants. One unit of activity corresponds to 1 μmoles of CO consumed per mg of $CODH_{Mt}$ per min.

	pH5.0	pH6.0	pH7.0	pH8.0	pH9.0	Averaged % activity relative to WT
Wild-type	16	43	100	170	300	100
$H124A_U$ ($H113A_{Mt}$)	8.0	19	50	70	110	44
$H127A_U$ ($H116A_{Mt}$)	2.2	2.8	3.2	5.3	6.6	6
$H130A_U$ ($H119A_{Mt}$)	5.0	0.1	35	50	79	27
$H133A_U$ ($H122A_{Mt}$)	0.71	0.5	5.2	2.7	6	3
H124A+ imidazole	-	19	52	65	-	45
H127A+ imidazole	-	1.0	3.0	5.0	-	3
$H127C_U$	9.5	19	48	69	120	46
$H127D_U$	0.1	0.2	0.4	0.6	1	0.4
$H124A_U$+ $H130A_U$	6.0	8.0	9.0	9.0	10	15
$H124A_U$+$H127A_U$+ $H130A_U$	0.0	0.0	0.0	0.0	0.0	0.0
$E126H_U$+ $H127A_U$	3.8	10	22	47	75	24
$H127A_U$+ $G128H_U$	0.28	0.33	0.64	0.84	1.3	0.8
$H133A_U$+ $A134H_U$	16	38	62	93	170	72
$A132H_U$+ $H133A_U$	2.30	4.7	10	18	34	11
$N300A_U$	6.4	26	39	58	94	41
$N300A_U$+$H130A_U$	4.8	15	42	66	103	36
$K725A_U$+$H124A_U$	0.1	0.3	0.7	1.3	2.5	0.7
$K725A_U$	-	-	-	73	-	42

Discussion

Proton Transfer Pathway in CODH

Our results suggest that His113, His116, His119, His122, Asn284 and possibly Lys587 are bases involved in proton transfer processes, supporting the initial proposal of Drennan *et al.* (*36*). The evidence is as follows. Firstly, these residues contain groups that could serve as general bases, they are conserved in most CODH's and are located roughly in a line between the C-cluster and the protein exterior. Their conserved nature extends beyond primary sequence, as illustrated in the structural comparisons shown in Figure 11. All of this is as would be expected, if these residues functioned as the bases used to abstract protons from the C-cluster (during CO oxidation) and to transfer those protons to solvent. Secondly, we found that replacing any of these residues with Ala diminished or abolished CO oxidation activities, and that effect was not due to protein misfolding or to the absence of metal centers in the proteins. Thirdly, activity could be rescued by replacing some of these residues with others that also have the capacity to serve as bases or by placing His residues in adjacent positions. We will assume such roles for the remainder of this discussion.

We initially assumed that protons would be transferred through a *linear* pathway where each residue of the pathway would be absolutely required (i.e. where replacing any member of the pathway with a residue that could not serve as a base would abolish activity). Although replacing His116 and His122 with Ala did essentially abolish

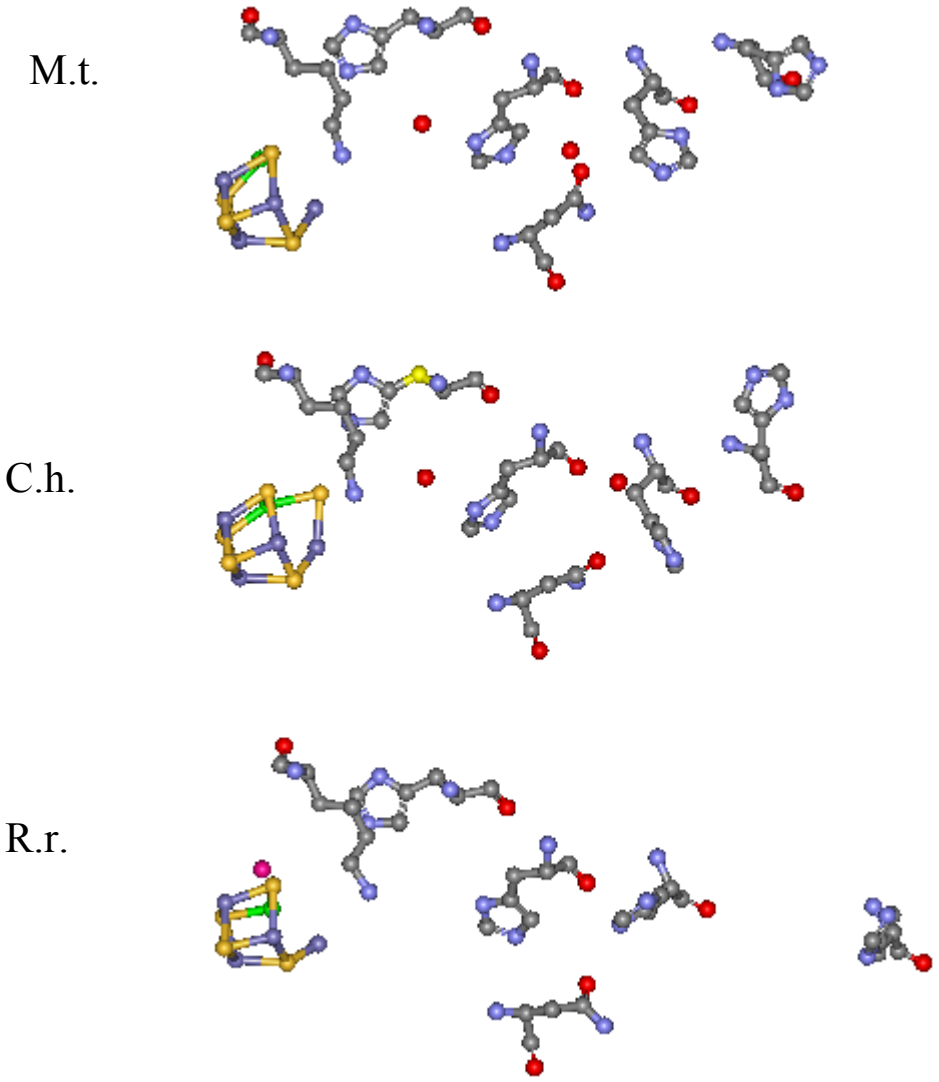

Figure 11: Proposed proton network in CODH. Alignment of proton network residues from published crystal structures. M.t. – *Moorella thermoacetica*, two structures are available (*37, 49*) and are indistinguishable in this region, shown is from (*49*). C.h. – *Carboxydothermus hydrogenoformans* (*35*). R.r. – *Rhodospirillum rubrum* (*36*).

activity, replacing others (His113 and His119) with Ala lowered activity but did not abolish it. The observed behavior suggests that protons are transferred through a *network* where some members of that network serve *redundant* roles and others serve *non-redundant* (or required) roles. Redundant bases would accept protons from a common donor and donate them to a common acceptor. The requirement for His116 and His122 suggests that they play non-redundant roles while the partial requirement for His113 and His119 suggests that they play redundant roles. These considerations constitute the foundation of our proton network model (Figure 12).

His113 is located nearest to the C-cluster, suggesting that it serves as the base used to abstract a proton from: a) water bound to the unique Fe during one step of catalysis; and from b) a Ni-bound carboxylate in another step of catalysis. However, the partially required nature of this residue suggests that another group might serve the same role. Lys587 is located near to the [Ni Fe] subsite of the C-cluster, and has been proposed to stabilize the Ni-bound carboxylate intermediate (36). The partial loss of activity in the mutant with this residue replaced with Ala is consistent with this proposal if the caveat that another group exists which plays a redundant role is included. The near-complete abolition of activity when Lys587 AND His113 were replaced with Ala is more dramatic than would be expected if both residues served separate functions with other redundant groups. In this case, the activity of the double-mutants would be the product of the activities of the individual mutants – namely 44 % × 42 % or 21 % of relative activity. The observed activity (0.7 %, relative to WT) suggests that His113 and

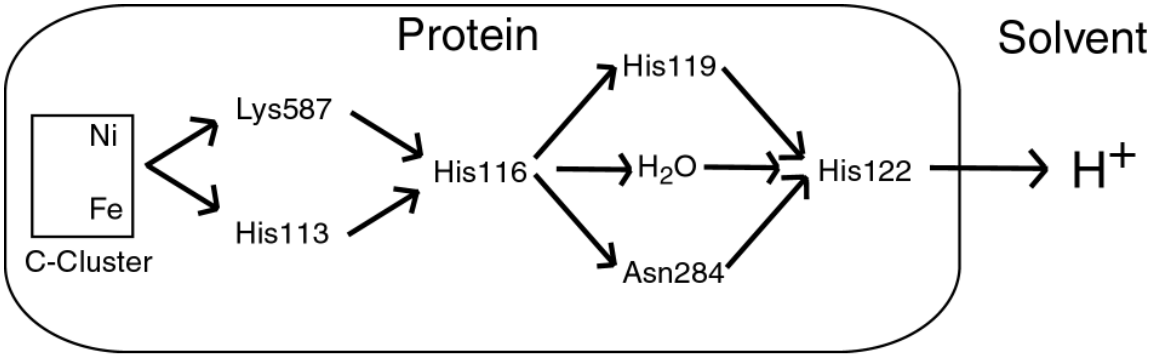

Figure 12: Proposed network scheme for $CODH_{Mt.}$

Lys587 serve the same function – i.e. they are an exclusive redundant pair. This suggestion is included in the model of Figure 11. Another possible redundant base to consider is water, in that there are two conserved water molecules within this region of the WT protein (35, 37, 49) and additional waters might be present in mutant proteins.

His116 is required for catalysis, and its location suggests that it accepts a proton from His113 (and from any redundant donor such as Lys587). According to our model, His116 donates a proton to either of three redundant acceptors, including His119, Asn284 and an unidentified acceptor, viewed in the model as one of the ordered waters present in the WT structure. We include a third redundant pathway to explain the substantial activity of the double mutant Asn284Ala:His119Ala. These three redundant groups then donate protons to His122, a required residue that appears to be non-redundant, and then His122 donates protons to solvent or an unidentified exogenous base.

Despite ambiguity as to some of the specific residues involved in this pathway, the location of those residues considered here indicates that *the proton transfer pathway is distinct from the electron transfer pathway* involving the B- and D-clusters. This distinction is illustrated in Figure 13. Similarly distinct proton and electron pathways are evident in the Ni hydrogenase from *Desulfovibrio gigas (12)* and in the iron-only hydrogenase from *Clostridium pasteurianum* (*56*). The former enzyme contains 4 His (3 of which are highly conserved) residues and a conserved Glu connecting the active site [NiFe] center to the surface; they apparently constitute a proton relay pathway. The location of this pathway differs significantly from the two Fe_4S_4 clusters and one Fe_3S_4 cluster used to transfer electrons between active site and surface. In the iron-only hydrogenase, electrons are transferred from the [Fe Fe] active site to the surface via Fe_4S_4 and Fe_2S_2 clusters, while protons are transferred via a free Cys residue, two Glu's, and a Ser (*56*). These similarities raise the possibility that separate proton and electron transfer pathways will be found whenever a series of Fe-S clusters constitute the electron transfer pathway.

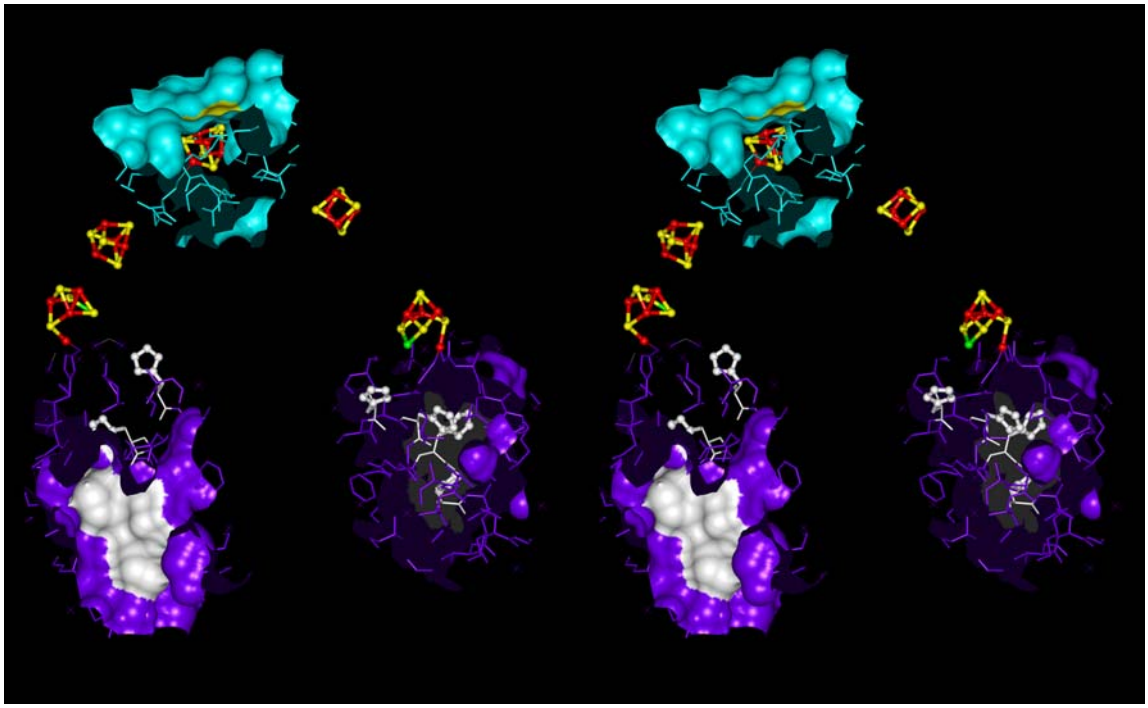

Figure 13: Stereoview showing distinct proton and electron transfer pathways through CODH.

CHAPTER IV

CONCLUSIONS AND POSSIBLE RESEARCH DIRECTIONS

Crystallization Studies

Five different forms of crystals of the α-subunit of CODH from *Moorella thermoacetica* were obtained, including a) cube-type crystals, b) a needle-type crystal, c) pentagonal or hexagonal crystals, d) cubic micro-crystals (not shown), and e) a rectangular crystal superimposed by a fiber or hair-like material. All of these diffracted to ~ 4 Å resolution. The quality and size of such crystals can be improved. These results indicate that good crystals of the α-subunit of CODH from *Moorella thermoacetica* can be obtained. A micro-crystal with a good shape can be chosen to obtain a single crystal for seeding, and can be added to a fresh drop of mixture of the α subunit and reservoir solution. Once optimal conditions have been obtained, crystallization of the α subunit in the present of substrates CO, CoA, and methyl group can be performed. Crystallization of various site-directed mutants of α subunit can also be performed. Structures of substrate-bound adducts of the enzyme and various mutants will aid immeasurably in deciphering the mechanism of catalysis (*46*).

The crystal structure of CODH/ACS_{Mt} with 1.9 Å resolution suggested two Ni containing A- clusters are catalytically active. The structure of the enzyme by Doukov *et al*. is equivalent to our closed conformation. Their A-clusters contain the same Ni_d site and $[Fe_4S_4]$ cube as we observe, but a Cu^+ ion replaces the Zn^{2+} of our A_c – cluster

and the Ni_p of our A_o- cluster. The conformation of one of the α subunits, to be called 'closed' (α_c) seems to be very similar to that reported by Doukov *et al*., while the other, to be called 'open' (α_o) has a larger exposed surface and allows the A-cluster greater accessibility to solvent. Based on calculation of the anomalous maps, we ruled out the presence of any significant amounts of Cu in our A-clusters.

However, we do not know why there are two different types of A-clusters in our crystals. Although we have the structure of the entire enzyme (CODH/ACS), there would still be an advantage to having a higher-resolution structure of α subunit. If we have better resolution of crystal structures of α subunits, we would be able to elucidate mechanisms of ACS_{Mt} in detail and to confirm our structures.

Mutational Studies

His 116_{Mt} and His 122_{Mt} are essential for the proton pathway as Drennan *et al.* proposed, while His 113_{Mt} and His 119_{Mt} are important, but not essential. Why are some conserved histidine residues essential for the proton relay and others are not? Is it possible that other residues take the role for some portion of the role of $H113_{Mt}$ and $H119_{Mt}$? To answer these questions, various mutants were made and their activities were checked.

We proposed a new network for the proton relay. By searching the structure in the Protein Data Bank and comparing sequence alignments, the conserved residues $K587_{Mt}$ and $N284_{Mt}$ can assume the roles of the conserved residues $H113_{Mt}$ and $H119_{Mt}$, respectively. $His116_{Mt}$ and $His122_{Mt}$ are essential for the proton network, but $His\ 113_{Mt}$, $Lys\ 587_{Mt}$, $His\ 119_{Mt}$, and $Asn284_{Mt}$ seem to be involved in the proton network, but not essential for catalysis. This suggests that protons are transferred through a network consisting of at least two linear pathways, all of which include $His116_{Mt}$ and $His122_{Mt}$. The proposed network were confirmed by checking the CO oxidation activity for the $Asn\ 284\ Ala_{Mt}$ mutant, $Lys587Ala_{Mt}$: $His113\ Ala_{Mt}$ double mutant, and $Asn\ 284\ Ala_{Mt}$: His119 Ala double mutant.

We note that CODH sequences that contain the conserved His, Lys and Asn residues which are involved in the proton pathway. Moreover, CODH sequences lacking the proton pathway residues; a horizontal line separates these two groups in Table 1. This implies that the proton pathway is either present or absent for a given protein. We propose that proteins lacking these residues (i.e. the sequences below the line in Table 1) are not enzymes that catalyze reaction [7] – i.e. they are not CODH's. Although further studies are required to examine this proposal, it is consistent with a report that cell extracts of one of the organisms which contain two of these below-the-line "CODH" enzymes (Clostridium acetobutylicum) do not exhibit CO oxidation activity (*57*)

REFERENCES

1. Ragsdale, S. W. and Kumar, M., (1996) *Chemical Rev. 87*, 2515-2539.
2. Hausinger, R. P., *Journal of Biological Inorganic Chemistry* (1997) *2*, 279-286.
3. Watt, R. K. and Ludden, P. W. (1999) *Cell. Mol. Life Sci. 56*, 604-625.
4. Maier,T., Jacobi, A., Sauter, M., and Bock, A. (1993) *J. Bacteriol. 175*, 630-635.
5. Colpasm, G. H., Brayman, T. G., Ming, L. J., and Hausinger, R. P. (1999) *Biochemistry 38*, 4078-4088.
6. Kerby, R. L., Ludden, P. W., and Roberts, G. P. (1997**)** *J. Bacteriol. 179*, 2259-2266.
7. Yokoi, K., Uthus, E. O., Nielsen, F. H. (2003) *Biol. Trace. Elem. Res*, *52*, 23-35.
8. Cengiz, D., Cokugras, A. N., Tezcan, E. F. (2003) *Biol. Trace. Elem. Res. 93*, 55-62.
9. Bagley, K. A., Garderen, C. J. V., Chen, M., Durin, E. C., Albracht, S. P. J. and Woodruff, W. H. (1994) *Biochemistry 33*, 9229-9236.
10. Surerus, K. K., Chen, M., Van der Zwaan, J. W., Rusnak, F. M., Kolk, M., Duin, E. C., Albracht, S. P. J., and Műnck, E. (1993) *Biochemistry 33*, 4980-4993.
11. Albracht, S. P. J. (1994) *Biochim. Biophys. Acta*, *1188*, 167-204.
12. Volbeda, A., Charon, M. H., Piras, C., Hatchikian, E. C., Frey M., and Fontecilla-Camps, J. C. (1995) *Nature 373*, 580-587.
13. Bagley, K. A., Durin, E. C., Roseboom, W., Albracht, S. P. J. and Woodruff, W. H. (1995) *Biochemistry 34*, 5527-5535.
14. Montet, Y., Volbeda, A., Piras, C., Hatchikian, E. C., Frey, M., Fontecilla-Camps, J. C., Pearson, M., Michel, L., Hausinger, R., and Karplus, P. A., (1996) *Biochemistry*

26, 8164-8172.

15. Higuchi, Y., Ogata, H., Hirota, S., Adachi, S., Yagi, T., and Yasuoka, N. (2002) *Acta Cryst.* A58 (Supplement), C247.

16. Rousset, M., Montet, Y., Guigliarelli, B., Forget, N., Asso, M., Bertrand, P., and Fontecilla-Camps, J. C. (1998) *Proc. Natl. Acad. Sci. U.S.A. 95*, 11625-11630.

17. Mobley, H. and Hausinger, R. (1989) *Microbiol. Revie*w *53*, 85-105.

18. Jabri, E. and Karplus, P. A., (1996) *Biochemistry 35*, 10616-10626.

19. Moncrief, M. B. and Hausinger, R. (1997) *Journal of Bacteriology*, *179*, 4081-4086.

20. Karplus, P. A., Pearson, M. A., and Hausinger, R. P. (1997) *Acc. Chem. Res. 30*, 330-337.

21. Mack, E. and Villars, D. S. (1923) *J. Am. Chem. Soc. 45*, 505-510.

22. Barrios, M. A. and Lippard, S. J. *J. Am. Chem. Soc*. (2000) *122* 9172-9177.

23. Jabri, E., Carr, M. B., Karplus, P. A., and Hausinger, R. (1995) *Science 268*, 998-1004.

24. Ermler, U., Grabarse, W., Shima, S., Goubeaud, M., and Thauer, R. K. (1997) *Science 278*, 1457-1462.

25. Ermler, U., Grabarse, W., Shima, S., Goubeaud, M., and Thauer, R. K., (1998) *Curr. Opin*. *Chem, Biol 8*, 749-758.

26. Thauer, R. K. (1998) *Microbiology 144*, 2377-2406.

27. Drake, H. L. (1994) Chapman & Hall, New York.

28. Rees, D. C. and Howard, J. B. (2003) *Science 300*, 929-931.

29. Anderson, M. E. and Lindahl, P. A. (1994) *Biochemistry 33*, 8702-8711.

30. Xia, J., Sinclair, J. F., Baldwin, T. O., and Lindahl, P. A. (1996) *Biochemistry 35*, 1965-1971.

31. Xia, J., Hu, Z., Popescu, C. V., Lindahl, P. A., and Műnck, E. (1997) *J. Am. Chem. Soc. 119*, 8301-8312.

32. Russell, W. K., Stålhandske, M.V., Xia, J., Scott, R. A., and Lindahl, P. A. (1997) *J. Am. Chem. Soc. 120*, 7502 –7510.

33. Hu, Z., Spangler, N, J., Anderson, M. E., Xia, J., Ludden, P. W., Lindahl, P. A., and Műnck, E. (1996) *J. Am. Chem. Soc. 118*, 830-845.

34. Anderson, M. E., DeRose, V. J., Hoffman, B. M., and Lindahl, P. A. (1993) *J. Am. Chem. Soc*. *115*, 12204-12205.

35. Dobbek, H., Svetlitchnyi, V., Gremer, L., Huber, R., and Meyer, O. (2001) *Science 293*, 1281-1285.

36. Drennan, C. L., Heo, J., Sintchak, M., Schreiter, E., and Ludden, P. W. (2001) *Proc. Natl. Acad. Sci. U.S.A. 98*, 11973-11978.

37. Doukov, T. I., Iverson, T. M., Seravalli, J., Ragsdale, S. W., and Drennan, C. L. (2002) *Science 298*, 567-572.

38. Loke, H. K., Bennett, G. N., and Lindahl, P. A. (2000) *P. Natl. Acad. Sci*. *U.S.A*. *97*, 12530-12535.

39. Loke, H. K., Tan, X., and Lindahl, P. A. (2002) *J. Am. Chem. Soc. 124*, 8667-8772.

40. Shin, W. and Lindahl, P. A. (1993) *Biochim. Biophy. Acta.* 1161, 317-322.

41. Duncan, E. M, (1993), *Practical Protein Crystallography*, 2nd ed., pp 1 – 20, Academic Press, New York.

42. Rhodes, G. (2000) *Crystallography Made Crystal Clear,* 2nd ed., Academic Press**,** New York.

43. Bergfors, T. M. (1999) *Protein Crystallization Techniques, Strategies, & Tips; a laboratory manual*, 2nd ed., pp 1-150, International University Line, La Jolla, CA.

44. Drenth, J. (1999) *Principles of Protein X-ray Crystallography*, 2nd ed., pp 1-18, Springer Verlag Publishing, New York.

45. Lundie, L. L. Jr. and Drake, H. L. (1984) *J. Bacteriol*. *159*, 700-703.

46. Barondeau, D. P. and Lindahl, P. A. (1997) *J. Am. Chem. Soc*. *119*, 3959-3970.

47. Maynard, E. L., Sewell, C., and Lindahl, P. A. (2001) *J. Am. Chem. Soc*. *123*, 4697-4703.

48. Bramlett, M. R., Tan, X., and Lindahl, P. A. (2003) *J. Am. Chem. Soc*. *125*, 9316-9317.

49. Darnault, C., Volbeda, A., Kim, E. J., Legrand, P., Vernede, X., Lindahl, P. A. and Fontecilla – Camps, J. C. (2003) *Nature Struct. Biol. Advanced Online Publication*.

50. Lindahl, P. A. (2002) *Biochemistry 41*, 2097-2105.

51. Feng, J., and Lindahl, P. A. (2003) *Biochemistry 43*, 1552-1559.

52. Lindahl, P. A., Münck, E., and Ragsdale, S. W. (1990) *J. Biol. Chem. 265*, 3873-3879.

53. Fraser, D. M., and Lindahl, P. A.(1999) *Biochemistry 38*, 15706-15711.

54. Lindahl, P. A. and Chang, B. (2001) *Origins of Life and Evolution of the Biosphere 31*, 403-434.

55. Pelly, J. W., Garner, C. W., and Little, G. H. (1978) *Anal. Biochem.* 86, 341-343.

56. Peters, J. W., Lanzilotta, W. N., Lemon, B. J., and Seefeldt, L. C. (1998) *Science 282*, 1853-1858.

57. Kim, B. H., Bellows, P., Datta, R., Zeikus, J.G. (1984) *Appl. Environ. Mocrobiol. 48*, 764-770.

VITA

EUN JIN KIM
103 F. Ken Nicolas Ave #B
College Station, TX 77840

EDUCATIONAL BACKGROUND

1999 – 2004	Texas A&M University, MS, Chemistry
1993 – 1995	Korea National University of Education, M.Ed., Chemistry
1989 – 1993	Korea National University of Education, B.S., Chemistry

PUBLICATIONS

1. Eun Jin Kim, Jian Feng, Matthew R. Bramlett, and Paul A. Lindahl, "Evidence for a Proton Transfer Pathway and for a Catalytically Required Persulfide Bond in Ni-Containing Carbon Monoxide Dehydrogenase." *Submitted to Biochemistry*.
2. Claudine Darnault, Anne Volbeda, Eun Jin Kim, Pierre Legrand, Xavier Vernède, Paul A. Lindahl, Juan C. Fontecilla-Camps "Ni-Zn-[Fe4-S4] and Ni-Ni-[Fe4-S4] clusters in closed and open α-subunits of acetyl-CoA synthase/carbon monoxide Dehydrogenase." (2003) *Nature Structural Biology 10*, 271 - 279
3. Dongwon you, Eunjin Kim, Sang Ook Kang, Jaejung Ko, and Seung Hee Lee, "Synthesis and Characterization of Palladium and Platinum Complexes of N,N'-Bis[2'(diphenylphosphino)phenyl1] Propane-1,3-Diamine. Single –Crystal Structures of [Pd($Ph_2PC_6H_4NC_3H_6NC_6H_4PPh_2$)] and [Pt($Ph_2PC_6H_4NH$)($SEt_2$)Cl." (1998) *Bulletin of the Korean Chemical Society 19*, No. 5.
4. Eun Jin Kim, " Synthesis and Characterization of 1,4-Diimine Complexes of Transition Metal." (1995) *Thesis of Master degree*.